Separation Science and Technology
Publication details, including instructions for authors and subscription information:
http://www.informaworld.com/smpp/title~content=t713708471

The Equilibrium Distribution Coefficient and Its Derivation from *TX* Solid-Liquid Equilibrium Diagrams

H. A. J. Oonk[a]; H. L. Pleijsier[a]
[a] LABORATORIUM VOOR ALGEMENE CHEMIE DER RIJKSUNIVERSITEIT UTRECHT, UTRECHT, THE NETHERLANDS

To cite this Article Oonk, H. A. J. and Pleijsier, H. L.(1971) 'The Equilibrium Distribution Coefficient and Its Derivation from *TX* Solid-Liquid Equilibrium Diagrams', Separation Science and Technology, 6: 5, 685 — 697

To link to this Article: DOI: 10.1080/00372367108057962

URL: http://dx.doi.org/10.1080/00372367108057962

SEPARATION SCIENCE, 6(5), pp. 685–697, October, 1971

The Equilibrium Distribution Coefficient and Its Derivation from *TX* Solid–Liquid Equilibrium Diagrams

H. A. J. OONK and H. L. PLEIJSIER

LABORATORIUM VOOR ALGEMENE CHEMIE DER RIJKSUNIVERSITEIT UTRECHT
VONDELLAAN 14
UTRECHT, THE NETHERLANDS

Summary

It is shown that in a binary system, in which the components form a series of mixed crystals, the equilibrium distribution coefficient at infinite dilution can be derived from the solid–liquid equilibrium diagram. For that purpose an expression is derived that relates the coefficient to the termodynamic properties of the system. The latter, in turn, are related to the solid–liquid equilibrium diagram by means of the equal-G curve. The practical operation of the method is illustrated with a number of examples for existing systems.

INTRODUCTION

The equilibrium distribution coefficient (k_0) plays a great part in zone refining (*1*, *2*). It is given by the ratio X_e^s/X_e^l where X_e^s and X_e^l are the equilibrium mole fractions of solute in solid and liquid phase, respectively.

This paper deals with distribution coefficients in binary systems in which a continuous series of mixed crystals can be formed. One of the main difficulties in these systems is to predict the value of k_0 for mole fractions approaching zero, i.e., to predict

$$k_0{}^0 \equiv \lim_{X_e{}^{s,l} \to 0} k_0 \qquad (1)$$

It is shown that, starting from the solid–liquid equilibrium diagram, reliable values for $k_0{}^0$ can be obtained by an extrapolation method based on thermodynamics.

The first two sections give a survey of the derivation of two limiting relations for dilute solutions: one originating from the equilibrium conditions for the solvent (first component), the other originating from the equilibrium conditions for the solute. The latter contains $k_0{}^0$ and its connection with the phase diagram is expressed with the help of the concept of equal-G curve (third section). The practical operation of the method is given (fourth section) and is demonstrated by a number of examples (fifth section).

GIBBS FUNCTIONS AND THERMODYNAMIC POTENTIALS

At constant pressure (we confine ourselves to isobaric, TX, equilibria) the Gibbs energy functions for solid and liquid solutions can be given as functions of absolute temperature and mole fraction of the second component, as

$$g^s(T, X^s) = g^{ids}(T, X^s) + g^{Es}(T, X^s) \tag{2}$$

$$g^l(T, X^l) = g^{idl}(T, X^l) + g^{El}(T, X^l) \tag{3}$$

The deviation from ideal behavior is expressed as an excess function, indicated by the superscript E.

For g^{id}, whether in solid or liquid solutions, we can write

$$g^{id}(T, X) = (1 - X)\mu_1{}^{\cdot}(T) + X\mu_2{}^{\cdot}(T) + RT\{(1 - X)\ln(1 - X) + X\ln X\} \tag{4}$$

The excess functions, which are by definition zero at the axes $X = 0$ and $X = 1$, are usually given as

$$g^E(T, X) = X(1 - X)f(T, X) \tag{5}$$

where $f(T, X)$ may vary from a constant to a rather complicated function of T and X.

To these mean molar Gibbs energies, partial molar Gibbs energies (thermodynamic potentials) are added (see Fig. 1), with the general relations

$$\mu_1 = g - X(\partial g/\partial X) \tag{6}$$

$$\mu_2 = g + (1 - X)(\partial g/\partial X) \tag{7}$$

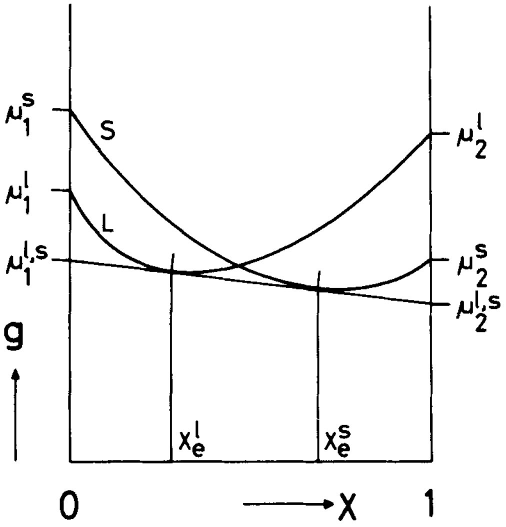

Fig. 1. Gibbs functions and thermodynamic potentials (l = liquid, s = solid) at a fixed temperature.

The conditions for equilibrium (Gibbs energy must be minimal for a given pressure, temperature, and over-all composition), are, in terms of the thermodynamic potentials,

$$\mu_1{}^s = \mu_1{}^l \tag{8}$$

$$\mu_2{}^s = \mu_2{}^l \tag{9}$$

LIMITING RELATIONS

Substitution of Eqs. (2) and (3), with Eq. (4), in Eqs. (6) and (7) gives the following equations for the thermodynamic potentials for solid and liquid

$$\mu_1{}^s(T, X^s) = \mu_1{}^{\cdot s}(T) + RT \ln (1 - X^s) + \mu_1{}^{Es}(T, X^s) \tag{10}$$

$$\mu_1{}^l(T, X^l) = \mu_1{}^{\cdot l}(T) + RT \ln (1 - X^l) + \mu_1{}^{El}(T, X^l) \tag{11}$$

$$\mu_2{}^s(T, X^s) = \mu_2{}^{\cdot s}(T) + RT \ln X^s + \mu_2{}^{Es}(T, X^s) \tag{12}$$

$$\mu_2{}^l(T, X^l) = \mu_2{}^{\cdot l}(T) + RT \ln X^l + \mu_2{}^{El}(T, X^l) \tag{13}$$

For $X \to 0$ the excess thermodynamic potentials become

$$\lim_{X\to 0} \mu_1{}^E = \lim_{X\to 0} [g^E - X(\partial g^E/\partial X)] = 0 \tag{14}$$

$$\lim_{X\to 0} \mu_2{}^E = \lim_{X\to 0} [g^E + (1 - X)(\partial g^E/\partial X)] = \lim_{X\to 0} (\partial g^E/\partial X) \tag{15}$$

According to Eqs. (14) and (15), the limiting value of $\mu_1{}^E$ is zero and that of $\mu_2{}^E$ is a constant. The nature of the excess functions is such that, with sufficient accuracy, these limiting values remain valid over the small X-range considered in the following derivations.

Now two relations for limiting behavior can be obtained; one based on Eq. (8), the equality of thermodynamic potentials for the solvent, and one based on Eq. (9) for the thermodynamic potentials for the solute.

Solvent

For $X \to 0$ the thermodynamic potentials become

$$\mu_1{}^s(T, X^s) = \mu_1{}^{\cdot s}(T) - RTX^s \tag{16}$$

$$\mu_1{}^l(T, X^l) = \mu_2{}^{\cdot l}(T) - RTX^l \tag{17}$$

Equating these expressions with condition (8) gives the following relation for the equilibrium mole fractions, indicated by the subscript e

$$\mu_1{}^{\cdot l}(T) - \mu_1{}^{\cdot s}(T) + RT(X_e{}^s - X_e{}^l) = 0 \tag{18}$$

or

$$\Delta\mu_1{}^{\cdot}(T) + RT(X_e{}^s - X_e{}^l) = 0 \tag{18'}$$

where $\Delta\mu_1{}^{\cdot}(T)$ can be written by $\partial\mu^{\cdot}/\partial T = -s^{\cdot}$ and, neglecting C_p influences, as

$$\Delta\mu_1{}^{\cdot}(T) = \Delta\mu_{1\,T=T_1} - \Delta s_1{}^{\cdot}(T - T_1) \tag{19}$$

which reduces to (as for the pure component 1, $\Delta\mu_1{}^{\cdot} = 0$ at $T = T_1$, its melting point)

$$\Delta\mu_1{}^{\cdot}(T) = -\Delta s_1{}^{\cdot}(T - T_1) \tag{20}$$

Substitution of Eq. (20) in Eq. (18′) gives

$$\boxed{X_e{}^s - X_e{}^l = \frac{(T - T_1)\Delta s_1{}^{\cdot}}{RT_1}} \tag{21}$$

where, in the denominator, T is replaced by T_1.

This relation, known as Van't Hoff's law, is the generic formula of a set of relations used to interpret temperature–time curves (melting curves) for the experimental determination of distribution coefficients; an example is given in Ref. *3* and a survey can be found in Ref. *4*.

Solute

For $X \rightarrow 0$ the thermodynamic potentials of the solute become

$$\mu_2^s(T, X^s) = \mu_2^{\cdot s}(T) + RT \ln X^s + \lim_{X \to 0} (\partial g^{Es}/\partial X) \tag{22}$$

$$\mu_2^l(T, X^l) = \mu_2^{\cdot l}(T) + RT \ln X^l + \lim_{X \to 0} (\partial g^{El}/\partial X) \tag{23}$$

Equating these expressions gives

$$\Delta\mu_2^{\cdot}(T) - RT \ln (X_e^s/X_e^l) + \lim_{X \to 0} (\partial/\partial X)\Delta g^E = 0 \tag{24}$$

which, by analogy to Eq. (20), reduces to

$$\Delta s_2^{\cdot}(T_2 - T) - RT \ln (X_e^s/X_e^l) + \lim_{X \to 0} (\partial/\partial X)\Delta g^E \tag{25}$$

And, because T approaches T_1 as X approaches zero, this yields for the distribution coefficient k_0^0, Eq. (1),

$$\boxed{\ln k_0^0 = \frac{\Delta s_2^{\cdot}(T_2 - T_1) + \lim\limits_{X \to 0} \dfrac{\partial}{\partial X} (\Delta g^E)_{T=T_1}}{RT_1}} \tag{26}$$

Unlike Eq. (21), the other limiting relation, Eq. (26) contains quantities for the whole binary system, of which, in this connection, $\lim (\partial/\partial X)\Delta g^E$ needs a further inspection. It is the difference in the initial slopes of the functions $g^{El}(X)$ and $g^{Es}(X)$, both taken at $T = T_1$. This difference can be derived from the TX diagram if we accept that our solid and liquid solutions can be described by the regular-solution model.

In the regular-solution approximation, g^E (Eq. 5) is taken to be independent of temperature, which implies, because

$$g^E = h^E - Ts^E \tag{27}$$

that s^E should be zero for all values of X (*5*).

In the case of molecules that form mixed crystals, for which the conditions are very stringent, it is generally believed, that s^E does not deviate appreciably from zero, at least in practical considerations. Consequently, Eq. (26) will be in the following form

$$\boxed{\ln k_0{}^0 = \frac{\Delta s_2{}^{\cdot}(T_2 - T_1) + \lim\limits_{X\to 0} \dfrac{d}{dX}\,\Delta h^E(X)}{RT_1}} \tag{28}$$

In the next section it is shown that the function $\Delta h^E(X)$ is related in a simple manner to the solid–liquid equilibrium diagram.

SOLID–LIQUID EQUILIBRIUM DIAGRAM; EQUAL-G CURVE

The Gibbs functions in the regular solution approximation are

$$\begin{aligned} g^s(T, X^s) &= (1 - X^s)\mu_1{}^{\cdot s}(T) + X^s\mu_2{}^{\cdot s}(T) \\ &\quad + RT\{(1 - X^s)\ln(1 - X^s) + X^s \ln X^s\} + h^{Es}(X^s) \end{aligned} \tag{29}$$

$$\begin{aligned} g^l(T, X^l) &= (1 - X^l)\mu_1{}^{\cdot l}(T) + X^l\mu_2{}^{\cdot l}(X) \\ &\quad + RT\{(1 - X^l)\ln(1 - X^l) + X^l \ln X^l\} + h^{El}(X^l) \end{aligned} \tag{30}$$

In Fig. 1 it is seen that the point of intersection of the two g-curves has a mole fraction that always lies between $X_e{}^l$ and $X_e{}^s$. Therefore, in the TX plane there is a curve connecting the points of intersection obtained at the various temperatures with the property that its path is always between solidus and liquidus. This curve, which is called equal-G curve (*6*, *7*), is given by

$$g^s(T, X) = g^l(T, X) \tag{31}$$

At the intersection $X^s = X^l = X$, so the superscripts in Eq. (31) can be dropped. Substitution of Eqs. (29) and (30) into Eq. (31) gives (with Eq. 20 and its equivalent for the second component) for the temperature of the equal-G curve

$$T_{\mathrm{EGC}}(X) = \frac{(1 - X)T_1\Delta s_1{}^{\cdot} + XT_2\Delta s_2{}^{\cdot} + \Delta h^E(X)}{(1 - X)\Delta s_1{}^{\cdot} + X\Delta s_2{}^{\cdot}} \tag{32}$$

Equation (32) contains the melting points and the melting entropies of the pure components and the function Δh^E; it can be written as

$$T_{\mathrm{EGC}}(X) = T_{\mathrm{ZERO}}(X) + \frac{\Delta h^E(X)}{(1 - X)\Delta s_1^{\cdot} + X\Delta s_2^{\cdot}} \tag{33}$$

with

$$T_{\mathrm{ZERO}}(X) = \frac{(1 - X)T_1\Delta s_1^{\cdot} + XT_2\Delta s_2^{\cdot}}{(1 - X)\Delta s_1^{\cdot} + X\Delta s_2^{\cdot}} \tag{34}$$

The curve in the TX plane represented by Eq. (34) is called zero line. In general this curve does not deviate much from the straight line connecting T_1 and T_2.

The distance from zero line to equal-G curve, at a given value X' of X, is equal to the value of the difference excess enthalpy for $X = X'$ divided by the mean entropy of melting at $X = X'$; see Fig. 2.

In the next section it will be shown how in an experimental phase diagram the equal-G curve can be drawn. If the equal-G curve is known, the function $\Delta h^E(X)$ can be calculated and from it $\lim_{X\to 0} (d/dX)\Delta h^E$, so that k_0^0 is known too (Eq. 28).

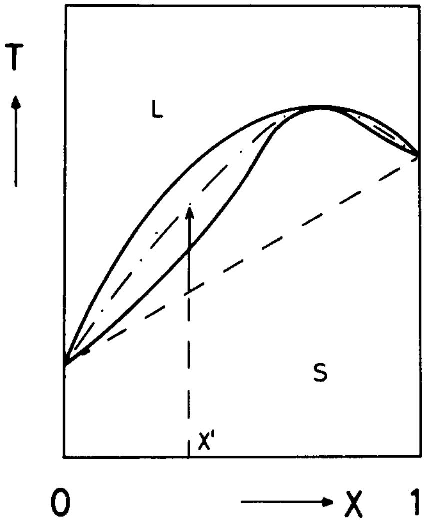

FIG. 2. Solid–liquid equilibrium diagram with equal-G curve (· –) and zero line (– –).

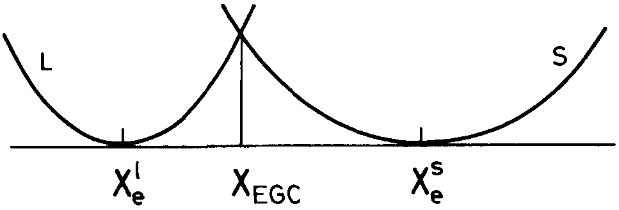

Fig. 3

APPROXIMATE EQUAL-G CURVE IN AN EXPERIMENTAL PHASE DIAGRAM

The procedure now is: To the experimental phase diagram a curve is added what is expected to be a good representative of the real equal-G curve (EGC). This approximate EGC, with Eqs. (33) and (34), gives the function $\Delta h^E(X)$. In practice a number of points of the approximate EGC are determined which give a number of values for $\Delta h^E(X)$. The initial slope of the function can then be found either graphically or arithmetically after adaptation of the values with the help of

$$\Delta h^E(X) = X(1 - X)\{A + B(1 - 2X) + C(1 - 2X)^2 + \cdots\} \quad (35)$$

The number of parameters A, B, C, . . . that should be adapted depends on the number and reliability of the individual values and on the nature of the function Δh^E.

In diagrams with narrow two-phase regions the approximate EGC can, with fair accuracy, be drawn at sight. For diagrams with broad two-phase regions the approximate EGC is found in the following way (see Fig. 3):

The abscissa of the point of intersection is, in general, at the side of that coexisting phase in which the corresponding Gibbs function has the greater degree of curvature, i.e., the greater value for the second derivative with respect to X. If, now, the position of X_{EGC} is given as a fraction

$$f \equiv \mathrm{abs}\left(\frac{X_{\mathrm{EGC}} - X_e^s}{X_e^s - X_e^l}\right) \quad (36)$$

then a good approximation appears to be

$$f = \tfrac{1}{2} - \tfrac{1}{5}\log_{10} Q \quad (37)$$

where

$$Q = \frac{(\partial^2 g^s/\partial X^2)_{X=X_e^s}}{(\partial^2 g^l/\partial X^2)_{X=X_e^l}} \tag{38}$$

For the separate solid and liquid states the second derivatives are given by

$$\frac{\partial^2 g}{\partial X^2} = \frac{RT}{X(1-X)} + \frac{d^2 h^E}{dX^2} \tag{39}$$

in which the first term on the right-hand side results from ideal-solution behavior; the second term is due to the deviation from that behavior when expressed in terms of the regular-solution model.

Unfortunately, the phase diagram only yields the function $\Delta h^E = h^{El} - h^{Es}$ and not h^{El} and h^{Es} separately, so that in principle the method should only be used if at least one of the separate functions is known from a different source. On the other hand, there are a great number of cases in which the first term of the right-hand side of Eq. (39) dominates. This is the more so in the regions close to the axes $X = 0$ and $X = 1$ which are, in view of the present method, the most important ones.

EXAMPLES

In this section the procedure is demonstrated with the help of four real systems. In two cases the approximate EGC was determined by the fraction method. For the other two the approximate EGC was drawn at sight. A survey of the results is given in Table 1. The inaccuracies of $\lim_{X\to 0} \Delta h^E$ given in the table are realistic estimates. The experimental values, also given in the table, were determined, by the authors referred to, with the help of melting curves based on Eq. (21).

(*a*) *Naphthalene* + *β-Naphtol* (*8*). The *TX* diagram of this system is shown by Fig. 4. The experimental data suggest solid and liquid solutions with small deviations from ideal-solution behavior. Moreover, these data were arrived at by a method that directly determines the corresponding coexisting phases (apart from the pure components, 8 pairs of coexisting phases are available). Consequently the conditions are ideal for the method based on the Eqs. (36), (37), and (38): both solid and liquid solutions can safely be taken as ideal.

The values calculated for Δh^E are shown in Fig. 5 along with the function obtained by the two-parameter adaptation of the 8 + 2 values.

TABLE 1

Survey of Calculations Made

					Solvent: lower melting component				Solvent: higher melting component			
System	T_1 (°K)	T_2 (°K)	$\Delta s_1^{\cdot}$ (cal mole^{-1} deg^{-1})	$\Delta s_2^{\cdot}$ (cal mole^{-1} deg^{-1})	Initial slope, $\Delta h^E(X)$	$\Delta s_2^{\cdot}$ $(T_2 - T_1)$	k_0^0, calc	k_0^0, exp	Initial slope, $\Delta h^E(X)$	$\Delta s_2^{\cdot}$ $(T_2 - T_1)$	k_0^0, calc	k_0^0, exp
(a)	355.3	395.5	12.84	13.68	−210	550	1.62		−150	−516	0.43	
					±20		±0.05		±20		±0.01	
(b)	342.5	398.6	17.3	18.1	−39	1015.4	4.2		59	−959.3	0.32	0.3
					±30		±0.2		±30		±0.01	Ref. *13*
(c)	304	314	9.2	9.2	−487	92	0.52		−1100	−92	0.15	0.14
												0.18
					±50		±0.04		±100		±0.02	Ref. *10*
(d)	145.2	174.3	1.2	0.8	60	22.4	1.33		−105	−35.2	0.67	0.675
					±10		±0.04		±15		±0.03	Ref. *3*

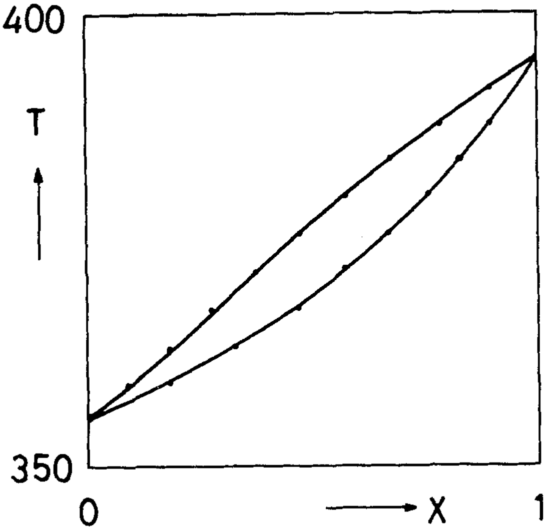

FIG. 4. Phase diagram of the system naphthalene + β-naphtol. (●) Experimental data (*8*). (——) Solidus and liquidus calculated.

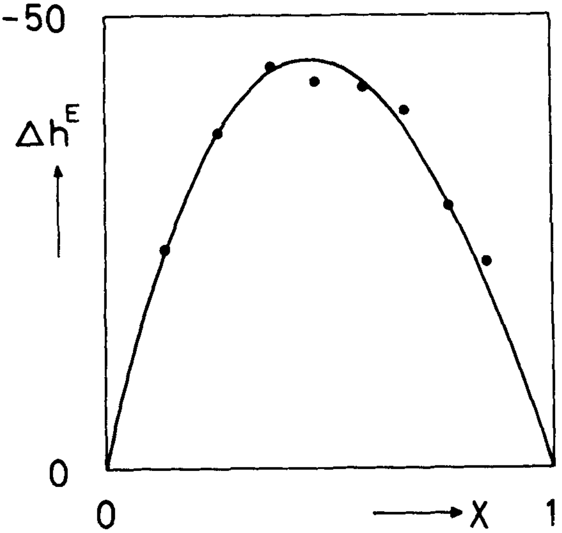

FIG. 5. The function $\Delta h^E/(X)$ for the system naphthalene + β-naphtol. (●) Calculated values. (——) Obtained by adaptation of those values.

The latter is $\Delta h^E(X) = -180X(1-X) - 30X(1-X)(1-2X)$. The result was checked by calculation (*7*) of the solid–liquid equilibrium diagram, putting $h^{El} = 0$ and $h^{Es}(X) = -\Delta h^E(X) = 180X(1-X) + 30X(1-X)(1-2X)$. The solidus and liquidus curves shown in Fig. 4 are those obtained by calculation; not the experimental ones.

(*b*) *Azobenzene* + *Stilbene* (*8*). Phase diagram of Type I according to the classification of Bakhuis Roozeboom (*9*). The same procedure was followed as under Case (a). There is good agreement between the experimental diagram and the one calculated.

(*c*) *Phenol* + *o-Cresol* (*10*). Phase diagram of Type III with narrow two-phase region. The EGC was drawn at sight. The four-parameter adaptation of the Δh^E values was calculated.

(*d*) 2,3- + 2,2-*Dimethylbutane* (*11*). Equilibrium between plastic-crystalline and liquid solutions. The phase diagram contains a maximum and a minimum. This type was not inserted by Bakhuis Roozeboom in his classification. In a recent enumeration (*12*) of types of phase diagrams, its code is [+ −].

The experimental diagram has a very narrow two-phase region due to the presence of two extrema and the very low values for the entropies of melting. The EGC was drawn at sight. The initial slopes were obtained by graphical processing of the Δh^E values.

LIST OF SYMBOLS

k_0	equilibrium distribution coefficient
k_0^0	equilibrium distribution coefficient at infinite dilution
X	mole fraction of the second component
T	absolute temperature
R	gas constant
g	Gibbs energy, molar
h	enthalpy, molar
s	entropy, molar
μ	partial Gibbs energy
T_1	melting point first component
T_2	melting point second component

Superscripts

id	referring to ideal-solution behavior
E	indicating excess functions

l	for the liquid state
s	for the solid state
dots	denoting specific molar quantities

Subscripts

1	for the first component, solvent
2	for the second component, solute
e	referring to thermodynamic equilibrium

The operator Δ written before a quantity or function denotes the difference between the values of that quantity or function in the liquid and in the solid state, in both states taken at the same mole fractions, e.g., $\Delta h_1^{\cdot} = h_1^{\cdot l} - h_1^{\cdot s}$.

Acknowledgment

The authors wish to express their thanks to Dr. N. J. G. Bollen for drawing their attention to the subject in connection with the k_0^0 of Sb in Bi (*14*).

REFERENCES

1. W. G. Pfann, *Zone Melting*, Wiley, New York, 1958.
2. H. Schildknecht, *Zone Melting*, Academic, New York, 1966.
3. S. V. R. Mastrangelo and R. W. Dornte, *J. Amer. Chem. Soc.*, *77*, 6200 (1955).
4. G. H. Vonkeman, "The Thermocouple Pt/Cr_2O_3/Pt and Its Use in Determining Melting Curves at Higher Temperatures, Ph.D. Thesis, University of Utrecht, Utrecht, The Netherlands, 1970.
5. J. H. Hildebrand and R. L. Scott, *Regular Solutions*, Prentice-Hall, Englewood Cliffs, New Jersey, 1962.
6. H. A. J. Oonk, *Rec. Trav. Chim. Pays-Bas*, *87*, 1345 (1968).
7. H. A. J. Oonk, *J. Chem. Educ.*, *47*, 227 (1970).
8. H. Vetter, S. Rössler, and H. Schildknecht, *Symposium über Zonenschmelzen und Kolonnenkristallisieren* (H. Schildknecht, ed.), Kernforschungsanstalt, Karlsruhe, Germany, 1963, p. 57.
9. H. W. Bakhuis Roozeboom, *Z. Phys. Chem.*, *30*, 385 (1899).
10. E. F. G. Herington and I. J. Lawrenson, *J. Appl. Chem.*, *19*, 337, 341 (1969).
11. H. L. Fink, M. R. Cines, F. E. Frey, and J. G. Aston, *J. Amer. Chem. Soc.*, *69*, 1501 (1947).
12. H. A. J. Oonk and A. Sprenkels, *Rec. Trav. Chim. Pays-Bas*, *88*, 1313 (1969).
13. M. J. van Essen, P. F. J. van der Most, and W. M. Smit, in *Purification of Inorganic and Organic Materials* (M. Zief, ed.), Dekker, New York, 1969, Chap. 21.
14. N. J. G. Bollen, M. J. van Essen, and W. M. Smit, *Anal. Chim. Acta*, *38*, 279 (1967).

Received by editor December 28, 1970